Acta Crystallographica Section F
Structural Biology and Crystallization Communications
ISSN 1744-3091

Expression, purification and crystallization of the ectodomain of the envelope glycoprotein E2 from *Bovine viral diarrhoea virus*

Oleg Iourin,[a] Karl Harlos,[a] Kamel El Omari,[a] Weixian Lu,[a] Jan Kadlec,[a]‡ Munir Iqbal,[b] Christoph Meier,[a] Andrew Palmer,[c] Ian Jones,[c] Carole Thomas,[d] Joe Brownlie,[d] Jonathan M. Grimes[a,e] and David I. Stuart[a,e]*

[a]Division of Structural Biology, Wellcome Trust Centre for Human Genetics, University of Oxford, Oxford OX3 7BN, England, [b]Institute for Animal Health, Compton Laboratory, Compton, Newbury, Berkshire RG20 7NN, England, [c]School of Biological Sciences, University of Reading, Reading RG6 6AJ, England, [d]Pathology, The Royal Veterinary College, Hawkshead Lane, North Mymms, Hatfield, Herts AL9 7TA, England, and [e]Science Division, Diamond Light Source Ltd, Diamond House, Harwell Science and Innovation Campus, Didcot OX11 0DE, England

‡ Current address: EMBL Grenoble, 6 Rue Jules Horowitz, 38042 Grenoble, France.

Correspondence e-mail: dave@strubi.ox.ac.uk

Received 5 November 2012
Accepted 29 November 2012

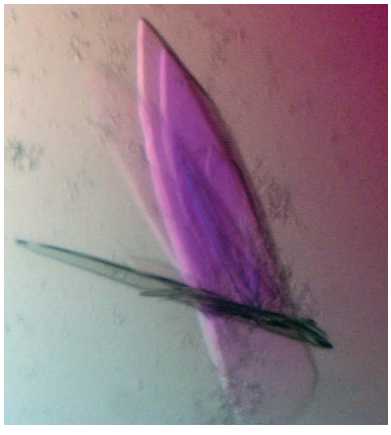

Bovine viral diarrhoea virus (BVDV) is an economically important animal pathogen which is closely related to *Hepatitis C virus*. Of the structural proteins, the envelope glycoprotein E2 of BVDV is the major antigen which induces neutralizing antibodies; thus, BVDV E2 is considered as an ideal target for use in subunit vaccines. Here, the expression, purification of wild-type and mutant forms of the ectodomain of BVDV E2 and subsequent crystallization and data collection of two crystal forms grown at low and neutral pH are reported. Native and multiple-wavelength anomalous dispersion (MAD) data sets have been collected and structure determination is in progress.

1. Introduction

Bovine viral diarrhoea virus (BVDV) is an economically important pathogen of cattle throughout the world and represents the prototype member of the *Pestivirus* genus from the *Flaviviridae* family (Lindenbach & Rice, 2001). Other economically important representatives from the genus are *Classical swine fever virus* (CSFV) and *Border disease virus* (BDV). Within the family, the *Hepacivirus* genus containing *Hepatitis C virus* (HCV) shares similarities with BVDV in terms of genome organization and translation strategy; thus, BVDV has been used as a model to study HCV (Buckwold *et al.*, 2003).

BVDV is an enveloped positive-stranded RNA virus of about 40–60 nm in diameter which contains four structural proteins: the nucleocapsid protein C and three glycoproteins E1, E2 and E^{rns}. E1 and E2 anchor the viral membrane at their C-terminus, while E^{rns} is loosely associated and exhibits RNAse activity (Lindenbach & Rice, 2001). E2 forms covalently disulfide-linked homodimers and heterodimers with E1 (Branza-Nichita *et al.*, 2001; Weiland *et al.*, 1990). The E1–E2 heterodimer is essential for virus entry, whereas E^{rns} is dispensable (Ronecker *et al.*, 2008; Wang *et al.*, 2004; Iqbal *et al.*, 2000).

The fusion machinery of pestiviruses and hepaciviruses is yet to be determined. Amongst the three currently recognized classes of viral fusion glycoproteins, both genera have been considered to have a class II fusion fold similar to the *Flavivirus* E and *Alphavirus* E1 proteins (Garry & Dash, 2003; Kielian, 2006). The class II fusion fold consists of three globular domains composed almost entirely of β-sheets. The identity of the fusion protein has not yet been established, but it is thought to be E2 (Krey *et al.*, 2010; Rümenapf *et al.*, 1993), although this is still debated (Garry & Dash, 2003; Pérez-Berna *et al.*, 2006). Pestiviral E2 glycoproteins are also the immunodominant surface glycoprotein and are the major target for virus-neutralizing antibodies (Weiland *et al.*, 1990; Wensvoort, 1989).

In view of the economic impact of BVDV, and pestiviruses in general, and the relationship between BVDV and HCV, we aimed to determine the structure of BVDV type-1 E2 (BVDV1 E2) by X-ray crystallography to gain insights into the fusion machinery of pestiviruses and hepaciviruses.

2. Materials and methods

2.1. Cloning

DNA encoding the ectodomain of BVDV1 E2 (strain Pe515, unpublished work) from residues 1–339 (corresponding to residues

Table 1
Primers used for cloning.

Constructs		Primers (5′–3′)
BVDV E2	*a*	CTGCACCGGTCACCTAGACTGCAAACCTGAAT
	b	CTGCGGTACCGTAATCCCGGTGATGGTCAGT
BVDV E2tr	*c*	CACGAAACCGGTTGCAAACCTGAATACTACTATGCCATAG
	d	GTGCTTGGTACCGTCAGTGACCTCCAGGTCAAAC
BVDV E2tr N117Q	*e*	GCCCATAGTAAGAGGGAAGTACCAGACAACACTGCTAAACGGACCGGC
	f	GCCGGTCCGTTTAGCAGTGTTGTCTGGTACTTCCCTCTTACTATGGGC
BVDV E2tr N186Q	*g*	CTCTATGATTGTATTCTTGGAGGACAGTGGACTTGTGTAACTGGGGAC
	h	GTCCCCAGTTACACAAGTCCACTGTCCTCCAAGAATACAATCATAGAG
BVDV E2tr N230Q	*i*	CATTGGCAAGTGTAGGCTGAAGCAGGAGACTGGCTACAGATTAGTAGAC
	j	GTCTACTAATCTGTAGCCAGTCTCCTGCTTCAGCCTACACTTGCCAATG
BVDV E2tr N239Q	*k*	GAGACTGGCTACAGATTAGTAGACCAGACTTCTTGCAATAGAGAGGGTGTG
	l	CACACCCTCTCTATTGCAAGAAGTCTGGTCTACTAATCTGTAGCCAGTCTC
BVDV E2tr N298Q	*m*	GTAGAAAAGACGGCATGTACCTTCCAGTACACAAAGACATTAAAGAATA
	n	TATTCTTTAATGTCTTTGTGTACTGGAAGGTACATGCCGTCTTTTCTAC

693–1031 of the polyprotein) was amplified from the plasmid pcDNA6-CD33-E2-1031-V5-His with the primers *a* and *b* (Table 1). The recombinant BVDV1 E2 expressed from this construct is biologically active as it can block BVDV infection (Pande *et al.*, 2005). Two mutations were found in the cDNA (Y9S and G94E); nevertheless these serine and glutamate residues are also present in different strains of BVDV, such as NADL 776263 and Ky1203. The insert was cloned in the pHLsec vector (Aricescu *et al.*, 2006) between the *Age*I and *Kpn*I restriction sites, resulting in a secreted protein with a C-terminal His_6 tag. A truncated version, BVDV1 E2tr, in which the first three and last five residues were deleted, was similarly produced (Fig. 1) using the PCR primers *c* and *d* (Table 1). Site-directed mutagenesis was performed to remove N-linked glycosylation from BVDV1 E2tr by replacing Asn with Gln at each of the predicted glycosylation sites (Fig. 1). Mutations were generated by two-step overlapping PCR using Pyrobest Polymerase (Takara) and the primers described in Table 1. PCR products were cloned into the pHLsec vector. All constructs were verified by DNA sequencing. In total, five point mutation constructs were produced (N117Q, N186Q, N230Q, N239Q and N298Q).

2.2. Protein expression and purification

Constructs coding for E2tr and its mutants were transiently expressed in HEK 293T cells in the presence of 5 µ*M* of the N-glycosylation inhibitor kifunensine (Toronto Research Chemicals, North York, Ontario, Canada; Chang *et al.*, 2007). The cell medium containing the secreted protein was harvested 4 d after transfection by centrifugation at 5000*g* at 288 K for 20 min to remove debris. The medium was filtered and incubated with Ni^{2+}-charged resin (FF Chelating Sepharose resin, GE Healthcare) in a shaking incubator for 90 min at 288 K. The resin was separated from the medium, washed with 20 m*M* Tris–HCl pH 8.0, 250 m*M* NaCl, 20 m*M* imidazole and eluted with the same buffer but containing 250 m*M* imidazole. In order to remove the C-terminal His-tag, the protein was separated from imidazole by size-exclusion chromatography in 15 m*M* Tris–HCl pH 7.8, 300 m*M* NaCl on a Superdex 200 column (S200 10/30, GE Healthcare) and incubated overnight at room temperature with Bovine Pancreas Carboxypeptidase A-Agarose (Sigma). The supernatant was then applied onto Ni^{2+}-charged resin to remove any residual His-tagged protein. 160 m*M* imidazole was added to the protein to keep it soluble before it was concentrated and incubated with GST-tagged Endo F1 enzyme overnight. The latter enzyme was removed by applying the mixture onto Fast Flow Glutathione Sepharose resin (GE Healthcare) pre-equilibrated with 20 m*M* Tris–HCl pH 8.0, 250 m*M* NaCl. Finally, proteins were further purified by size-exclusion chromatography in 20 m*M* Tris–HCl pH 8.0, 250 m*M* NaCl on a Superdex 200 column. Fractions containing pure E2 protein were pooled and 3-(1-pyridino)-1-propane sulfonate (NDSB-201, Soltec Ventures Inc.) was added to a final concentration of 300 m*M* in order to facilitate concentration of the samples to between 3.6 and 10 mg ml^{-1}.

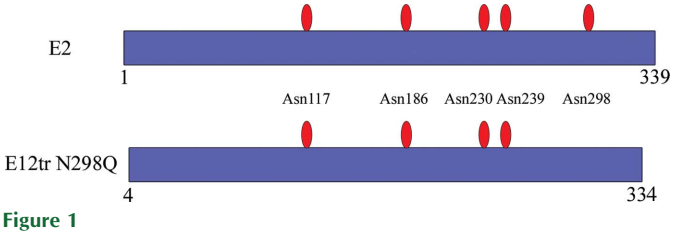

Figure 1
Schematic representation of the BVDV E2 constructs which produced quality diffracting crystals. Predicted glycosylation sites are marked as red ovals.

The same protocol was followed to express and purify nontruncated E2 and the selenomethionine derivative of the mutant E2tr N298Q, apart from the following alterations: the C-terminal His tag was not removed from BVDV1 E2 and for E2tr N298Q *in vivo* selenomethionine incorporation was performed according to previously reported work (Aricescu *et al.*, 2006) with the alteration that the original medium was replaced with medium supplemented with 0.2 m*M* selenomethionine 24 h after transfection.

2.3. Crystallization and data collection

Crystals of E2 and E2tr N298Q were grown by sitting-drop vapour diffusion at 294 K in 96-well plates (Greiner Bio-One Ltd, Stonehouse, England) by a Cartesian Technologies MIC4000 robot, as described previously (Walter *et al.*, 2005). BVDV1 E2 was concentrated to 3.8 mg ml^{-1} and crystallized in Grid Screen PEG 6000 (Hampton Research) condition C2 (20% PEG 6000, 0.1 *M* citric buffer pH 5.0). This condition was further screened using a variation of the three-row optimization technique (Walter *et al.*, 2005) in which the reservoir solution was diluted over the range 67–100% in 3% steps and drops were set up at 1:1, 2:1 and 1:2 protein:reservoir drop ratios. From these results, the best crystals were observed at a reservoir-solution dilution of 79% and a 2:1 protein:reservoir drop ratio. Adding magnesium sulfate to the reservoir solution at a final concentration of 20 m*M* further improved the crystal quality. Plate-like crystals grew to approximate dimensions of 400 × 50 × 5 µm (Fig. 2). Selenomethionine-labelled BVDV1 E2tr N298Q crystallized at a concentration of 9.7 mg ml^{-1} in Grid Screen MPD (Hampton Research) condition D5 [65% methyl-2,4-pentanediol (MPD), 0.1 *M* Tris pH 8.0]. The best crystals were obtained by mixing the following reservoir solutions in a 1:1 ratio: 65% MPD, 0.1 *M* Tris pH 8.0 with

Table 2
Data-collection and processing statistics.

Values in parentheses are for the highest resolution shell.

		E2tr N298Q			
	Native E2	High resolution	Peak	Inflection	Remote
Beamline	I24	I02	I03	I03	I03
Space group	$P2_12_12$	$C2$	$C2$	$C2$	$C2$
Unit-cell parameters (Å, °)	a = 160.7, b = 49.7, c = 136.4	a = 132.2, b = 47.6, c = 159.3, β = 108.2	a = 133.2, b = 47.8, c = 154.7, β = 110.8	a = 133.2, b = 47.8, c = 154.7, β = 110.8	a = 133.2, b = 47.8, c = 154.7, β = 110.8
Wavelength (Å)	1.0341	0.9796	0.9794	0.9796	0.9686
Resolution (Å)	50–3.3	50–2.6	50–3.1	50–3.4	50–3.3
No. of unique reflections	17239 (1659)	29885 (2320)	16339 (1075)	13221 (545)	14284 (348)
No. of observed reflections	83948	148705	131000	42235	45314
Completeness (%)	99.9 (99.8)	97.0 (76.1)	96.2 (63.3)	99.9 (100)	99.9 (100)
Multiplicity	4.9 (4.8)	5 (4.5)	8 (2.7)	3.2 (1.9)	3.2 (1.9)
$\langle I/\sigma(I)\rangle$	6.6 (1.5)	15.1 (1.7)	17.9 (2.1)	12.1 (2.0)	12.4 (2.1)
$R_{\rm merge}$† (%)	24.2 (92.2)	11.0 (100)	12.1 (27.6)	11.3 (24.7)	11.6 (23.3)

† $R_{\rm merge} = \sum_{hkl}\sum_i |I_i(hkl) - \langle I(hkl)\rangle| / \sum_{hkl}\sum_i I_i(hkl)$, where $I_i(hkl)$ is the ith measurement and $\langle I(hkl)\rangle$ is the weighted average of all measured reflections.

40% MPD, 0.1 *M* Tris pH 8.0. The optimized crystallization condition of 52.5% MPD, 0.1 *M* Tris pH 8.0 gave crystals of approximate dimensions 350 × 110 × 5 µm (Fig. 2).

Crystals of BVDV1 E2 were flash-cooled in liquid nitrogen using 25%(*v*/*v*) glycerol/reservoir solution as cryoprotectant, whereas crystals of selenomethionine-labelled E2tr N298Q were cooled without additional cryoprotection. Data sets were recorded from crystals at 100 K on beamlines I24, I02 and I03 at the Diamond Light Source (Didcot, England) and were processed with *HKL*-2000 (Otwinowski & Minor, 1996). Processing statistics are summarized in Table 2.

3. Results and discussion

A secretory mammalian expression system was used for expressing BVDV1 E2 since it contains a total of 17 cysteines involved in intramolecular and intermolecular disulfide bonds. As expected E2 was expressed as a covalently bound homodimer; however, its glycosylated form failed to crystallize. Proteins were then treated with endoglycosidase F1 to cleave glycosidic bonds of N-linked sugars within the di-*N*-acetylchitobiose core. Following deglycosylation, E2 had a tendency to precipitate upon concentration and NDSB-201 was added to increase solubility. Typically, 3.5 mg pure protein was obtained per litre of cell culture for both BVDV1 E2 and E2tr constructs, although substantially less selenomethionine-labelled protein was expressed.

BVDV1 E2 crystallized at pH 5 and diffracted to a resolution of 3.3 Å at best in space group $P2_12_12$ with unit-cell parameters a = 160.7, b = 49.7, c = 136.4 Å, but crystal diffraction was not reproducible, which consequently made experimental phasing and resolution improvement difficult. A new construct was designed in which the N- and C-terminal predicted disordered regions were deleted (E2tr). Additionally, five constructs were made, each bearing a mutation on one of the five predicted glycosylation sites. The latter mutants were expressed to similar levels as the wild type apart from E2tr N186Q, for which expression was negligible. The mutant E2tr N298Q gave reproducible crystals at pH 8 and allowed a selenomethionine multiple-wavelength anomalous dispersion (MAD) data set to be collected from a single crystal. A second crystal was used to collect a higher resolution data set (2.6 Å), determined by requiring $\langle I/\sigma(I)\rangle$ to be above 1.5 in the highest-resolution shell. The unit-cell parameters are related to those of the low-pH form, a = 133.2, b = 47.8, c = 154.7 Å, β = 110.8°, but the space group in this case is $C2$. Based on these data, the asymmetric units of both crystal forms are likely to contain two or three monomers, corresponding to solvent contents of 65 or 48% and of 61 or 41%, for the $P2_12_12$ and $C2$ space groups, respectively.

The structure of BVDV1 E2 will greatly help our understanding of the pestiviral fusion machinery and also help with the design of improved neutralizing antibodies for BVDV and for pestiviruses in general, since E2 is well conserved within the genus. In addition the

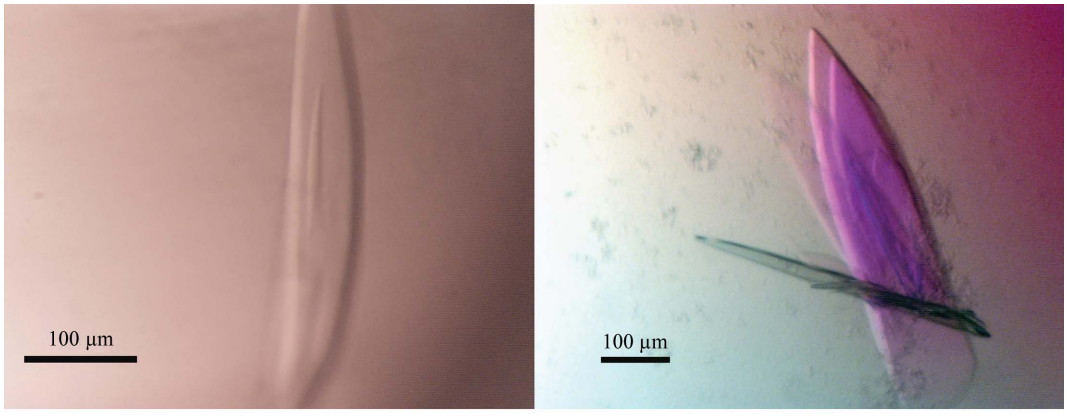

(*a*) (*b*)

Figure 2
Typical BVDV E2 crystals. (*a*) Crystal belonging to space group $P2_12_12$ (BVDV E2 construct). (*b*) Crystals belonging to space group $C2$ (BVDV E2tr N298Q construct).

structure may throw light on the relationship between BVDV and human pathogen HCV.

Tom Walter and Geoff Sutton are thanked for valuable technical assistance. We thank the staff of beamlines I02, I03 and I24 at the Diamond Light Source synchrotron for technical support. The work was supported by the UK MRC. The Wellcome Trust is acknowledged for providing administrative support (grant No. 075491/Z/04).

References

Aricescu, A. R., Lu, W. & Jones, E. Y. (2006). *Acta Cryst.* D**62**, 1243–1250.
Branza-Nichita, N., Durantel, D., Carrouée-Durantel, S., Dwek, R. A. & Zitzmann, N. (2001). *J. Virol.* **75**, 3527–3536.
Buckwold, V. E., Beer, B. E. & Donis, R. O. (2003). *Antiviral Res.* **60**, 1–15.
Chang, V. T., Crispin, M., Aricescu, A. R., Harvey, D. J., Nettleship, J. E., Fennelly, J. A., Yu, C., Boles, K. S., Evans, E. J., Stuart, D. I., Dwek, R. A., Jones, E. Y., Owens, R. J. & Davis, S. J. (2007). *Structure*, **15**, 267–273.
Garry, R. F. & Dash, S. (2003). *Virology*, **307**, 255–265.
Iqbal, M., Flick-Smith, H. & McCauley, J. W. (2000). *J. Gen. Virol.* **81**, 451–459.
Kielian, M. (2006). *Virology*, **344**, 38–47.
Krey, T., d'Alayer, J., Kikuti, C. M., Saulnier, A., Damier-Piolle, L., Petitpas, I., Johansson, D. X., Tawar, R. G., Baron, B., Robert, B., England, P., Persson, M. A., Martin, A. & Rey, F. A. (2010). *PLoS Pathog.* **6**, e1000762.
Lindenbach, B. D. & Rice, C. M. (2001). *The Pestiviruses.* Philadelphia: Lippincott Williams & Wilkins.
Otwinowski, Z. & Minor, W. (1996). *Methods Enzymol.* **276**, 307–326.
Pande, A., Carr, B. V., Wong, S. Y. C., Dalton, K., Jones, I. M., McCauley, J. W. & Charleston, B. (2005). *Virus Res.* **114**, 54–62.
Pérez-Berna, A. J., Moreno, M. R., Guillén, J., Bernabeu, A. & Villalaín, J. (2006). *Biochemistry*, **45**, 3755–3768.
Ronecker, S., Zimmer, G., Herrler, G., Greiser-Wilke, I. & Grummer, B. (2008). *J. Gen. Virol.* **89**, 2114–2121.
Rümenapf, T., Unger, G., Strauss, J. H. & Thiel, H. J. (1993). *J. Virol.* **67**, 3288–3294.
Walter, T. S. *et al.* (2005). *Acta Cryst.* D**61**, 651–657.
Wang, Z., Nie, Y., Wang, P., Ding, M. & Deng, H. (2004). *Virology*, **330**, 332–341.
Weiland, E., Stark, R., Haas, B., Rümenapf, T., Meyers, G. & Thiel, H. J. (1990). *J. Virol.* **64**, 3563–3569.
Wensvoort, G. (1989). *J. Gen. Virol.* **70**, 2865–2876.